Elastic and Tensile Properties of Aromatic Polyamideimide Composite Films with Aromatic Polyamide Fiber Reinforcements Having Various Textures and Fiber Orientations

YOSHIHIRO OHMIYA and HIROTARO KAMBE, *Institute for Composite Materials, Faculty of Technology, Gunma University, 1-5-1 Tenjincho, Kiriu 376, Japan*

Synopsis

Aromatic polyamideimide (PAI) films were reinforced with aromatic polyamide fiber (DuPont, Kevlar 49) as unidirectional composite (type I), bidirectional laminate composite (type II), and bidirectional cloth composite (type III). The elastic and tensile load-elongation properties of composite films at ambient temperature were investigated with respect to fiber orientation. The properties of the type I composite film are more anisotropic than those of other composite films. But, for the type I composite film, the most significant effect of the reinforcement fiber is observed at the fiber direction. With bidirectional reinforcement (types II and III) the anisotropy of the composite is reduced, but the strengths at the fiber directions are depressed markedly by the existence of the fibers of the other orientations.

INTRODUCTION

The composite of a plastic with a continuous fiber is generally reinforced with a unidirectional fiber orientation. The unidirectionally reinforced composite, however, exhibits strong anisotropy in its properties. For the purpose of producing a more isotropic composite, it is often more desirable to use the reinforcement with laminarly crossed fibers or with a cloth.

A thermally stable, flexible film of an aromatic polyamideimide is obtained by casting from a solution in a polar solvent. The dynamic mechanical properties of a polyamideimide film reinforced with carbon fiber was investigated by Kambe et al.[1] The dynamic elastic properties of carbon fiber composite are essentially controlled by fiber orientations. At the orientation of fibers parallel with a stress direction, the composite behaves similarly as a carbon fiber bundle. The carbon fiber composite is a very hard plastic with a minute flexibility.

The more flexible film is obtained with a soft fiber reinforcement. An aromatic polyamide fiber may be used as a more flexible reinforcement without loss of thermal stability of an aromatic polyamideimide composite film. The fracture toughness of a composite of an epoxy resin reinforced with an aromatic polyamide fiber was investigated by Mai and Catino.[2] They studied the effects of controlled interfacial bonding between fiber and matrix resin. These composites were brittle, even though they used a flexible fiber reinforcement.

Journal of Applied Polymer Science, Vol. 32, 4735–4749 (1986)

CCC 0021-8995/86/044735-15$04.00

The anisotropy of mechanical properties of unidirectionally reinforced composite materials has been investigated by Nielsen,[3] Tsai and Harn,[4] and others. The dependence of mechanical properties of composite materials on the orientation angle, i.e., the angle between fiber axis and tensile load axis extensively investigated. Tsai[5] indicated the role of reinforcing fibers is different for each range of orientation angle.

In the present investigation, a fiber-reinforced aromatic polyamideimide film of significant flexibility and strength was obtained by keeping a suitable range of volume fraction of reinforcing aromatic polyamide fibers. The anisotropy of mechanical properties is mostly dependent on the orientation of reinforcing fibers. Three types of composite with different reinforcement textures were used as samples. We measured the stress relaxation and tensile load–elongation behaviors of fiber-reinforced composite films at ambient temperatures. The dependence of these mechanical properties on the fiber orientation angle is investigated with respect to the various reinforcement textures. The role of reinforcing fibers is discussed.

EXPERIMENTAL

Materials

An aromatic polyamideimide varnish produced experimentally by the Film Laboratory of Toray Co., was kindly supplied us to use as a material. The chemical formula of the present sample of polyamideimide (PAI) is as follows:

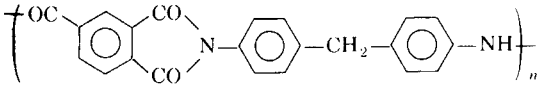

Dimethylacetamide was used as a solvent in varnish and was used as a diluent.

A commercial fiber of an aromatic polyamide, Kevlar 49, was obtained from DuPont in a form of 195 denier yarn, and was used as a reinforcement. Kevlar has the following chemical structure:

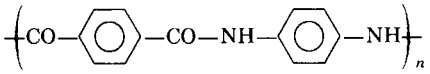

REINFORCEMENT TEXTURES

Three types of composite film with different reinforcement textures were prepared as shown in Table I. The type I composite film was produced with a unidirectional reinforcement of Kevlar yarn. The type II composite was with bidirectional reinforcement of a laminate of prependicularly crossed Kevlar yarns. In type I and II composites, Kevlar 49 yarn was used as received.

The type III composite was reinforced with a bidirectional plein cloth. A cloth of Kevlar 49 was woven by the following procedures. For the sake of weaving, Kevlar yarns were twisted to increase ultimate load–elongation characteristics in tension. In Figure 1, the ultimate load and elongation are shown against the number of twist per length. The ultimate load shows a maximum at a twist of 250 turns/m and the ultimate elongation does not change markedly up to the twist of 500/m. Then, we twist Kevlar yarns

TABLE I
Sample Composite Films

Type	Reinforcement	Twist (m^{-1})	Fiber density (yarns/cm)	PVA Sizing	Volume fraction of fibers (%)
I	Unidirectional yarns	No	10	No	5 ± 1
II	Bidirectional layered crossed yarns	No	Longitudinal 10 Transverse 10	No	10 ± 2
III	Bidirectional plein cloth	200 Clockwise	Warp 10 Woof 8	Yes No	9 ± 2

clockwise by 220 turns/m for use as the warp of sample cloth. Twisted Kevlar yarns were sized by dipping in a 3% poly (vinylalcohol) (PVA) solution. The yarns used for the woof were not sized to prevent the slip between yarns during weaving. The yarns were woven to a cloth by using a weaving machine at the Gunma Prefectural Textile Research Institute in Kiriu. According to the machine conditions, the density of the sized warp was 10 yarns/cm and that of the unsized woof was 8 yarns/cm.

Casting Films

The PAI composite films were prepared as follows. First, the fiber reinforcement was fixed on glass plate. For type I and II composites, the Kevlar yarns were wound up around the glass plate at a definite separation of ca. 1 mm. Along the edge of the glass plate, the fibers were fixed with adhesive. For type III composite, a cloth was fixed on a flat plane of the glass plate by cellophane tapes. In preparing the type III composite, it was necessary to remove the PVA sizing before putting in the resin. For this purpose, the cloth on the glass plate was immersed in water overnight and, then, dried up in a desiccator to remove water completely.

The fiber reinforcement was dipped in the PAI varnish together with the glass plate and dried in vacuum overnight. After leaving in air for several hours, the resulting film was heated at 140°C for 3 h at ambient pressure. The film was removed from the glass plate and heated at 250°C in vacuum for 3 h

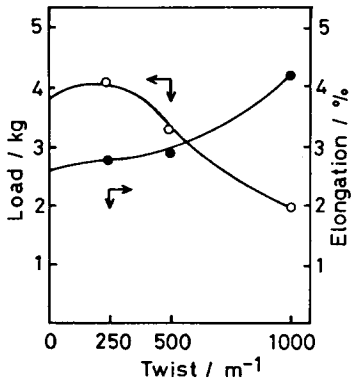

Fig. 1. Dependence of ultimate load (○) and elongation (●) of Kevlar 49 yarns on twist.

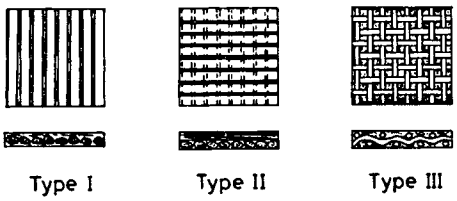

Fig. 2. Schematic models of composite films.

to get a sample film. From the infrared absorption spectra, no existence of the effect of oxidation and the remaining solvent was confirmed for this preparation process.

Composite Film Sample

By these procedures, the obtained composite films a considerable flexibility and an enhanced strength compared with the original PAI film. The schematic models of these three types of the composite film are shown in Figure 2.

In type I and II composites, the nontwisted yarns are somewhat swollen and intermixed with PAI matrix without clearly indicating the boundaries between fiber and resin. In type III composite, the yarns are compactly twisted and undulated in the matrix. The boundaries between fibers and resin are more easily seen in this type than in other types.

The volume fraction of the reinforcement in the composite film was evaluated from the density of the film as shown in Table I.

Measuring Methods

The stress–relaxation of the composite film was measured with a home-built stress–relaxation apparatus.[6] After giving an initial extension of 0.4% instantaneously, the stress change of a rectangular sample strip of 25 × 5 mm was followed at an ambient atmosphere. The minute strain confirms a linear response of the sample specimen. The tensile stress was measured by a Toyo-Baldwin strain-gauge sensor at a fixed interval of logarithmic time during a period from 0.1 to 10^4 s by using a Logtimer, supplied by the courtesy of Japan Synthetic Rubber Co. The stress data was digitized and stored in the Logtimer automatically, and was input into a personal computer Nippon Electric Co. PC-8801 and processed to give a relationship of logarithmic Young's modulus, log E, against logarithmic time, log t.

The load–elongation of the composite films was measured by a Toyo-Baldwin Tensilon. The specimens were a length of 20 mm constantly and widths of 5, 10, 15, and 20 mm at various fiber orientation angles. Tension testing was a rate of elongation of 5 mm/s at an ambient atmosphere.

RESULTS AND DISCUSSION

Elastic Properties

The stress–relaxation curves obtained for Kevlar 49 yarns and a PAI homogeneous film are shown in Figure 3. The initial Young's modulus of

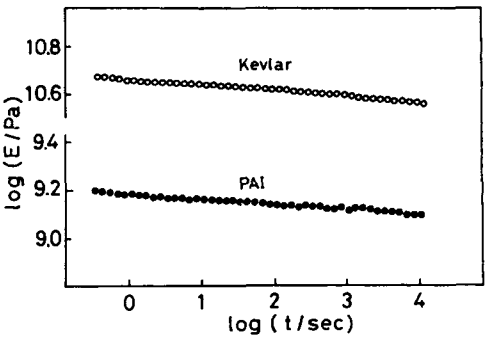

Fig. 3. Relaxation curves for Kevlar 49 yarns and PAI film.

Kevlar (Ef) is 5×10^{10} Pa and that of PAI (Em) is 1.6×10^{9} Pa. The ratio of initial Young's moduli E_f/E_m is 31. The relaxation curves of both samples are linear for these plots, indicating non-relaxing behaviors of these materials.

The stress–relaxation curves for uniaxially reinforced type I composite at the different fiber orientation angles θ are shown in Figure 4. The greatest initial Young's modulus is observed at $\theta = 0°$, indicating that the elastic property of the type I composite at $\theta = 0°$ is mainly governed by the existence of reinforcing fibers.

The relaxation behavior of type I composite observed at $\theta = 0°$ is also controlled by Kevlar fibers and is not significant. The relaxation is enhanced with increasing θ, and at $\theta = 90°$, in particular, a very marked relaxation is observed. This behavior can be explained by the strain additivity of a series model of composite materials. The relaxations of easily relaxable resin parts are accumulated in series to give an enlarged overall relaxation behavior.

In Figure 5 are shown the stress–relaxation curves of the type II bidirectionally reinforced laminate composite at various fiber orientation angles. This composite is constituted from two orthogonally oriented unidirectional plates at $\theta = 0°$ and 90° and shows relaxation curves symmetrically situated around a curve at $\theta = 45°$. At $\theta = 0°$ and 90°, the direct effects of Kevlar fibers appear in high modulus and little relaxation. At the other θ's, the difference in modulus is marked but no significant difference in relaxation behavior is observed in contrast to type I composite shown in Figure 4.

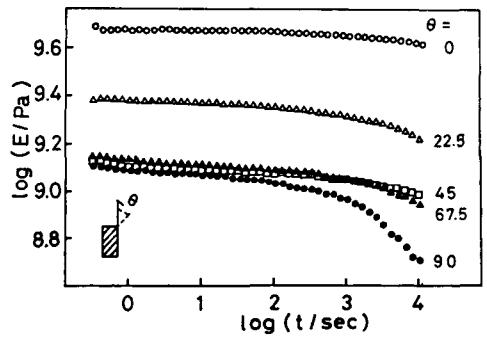

Fig. 4. Relaxation curves for type I composite at various fiber orientation angles.

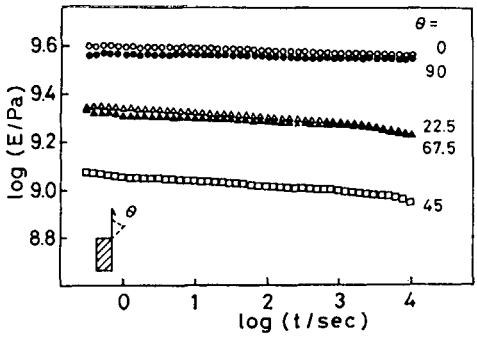

Fig. 5. Relaxation curves for type II composite at various fiber orientation angles.

Another feature of the bidirectional reinforcement is that the initial modulus is lower in general than that of the unidirectional one.

The stress–relaxation curves obtained for the type III bidirectionally reinforced composite with a cloth of Kevlar 49 are shown in Figure 6. The greatest initial Young's modulus is found at the orientation angle $\theta = 0°$. The modulus at $\theta = 90°$ is next to that at $\theta = 0°$. The modulus is greater when the fiber axis lies parallel to the load axis, but because of the difference of the fiber density of warp and woof in the cloth shown in Table I, the modulus at $\theta = 0°$ and 90° are not exactly the same. At various θ's, the relaxation curves show a similar tendency, though the relaxation behaviors are not truly symmetrical at angles for both sides of $\theta = 45°$. The isotropic character of the stress–relaxation is enhanced by a cloth reinforcement.

Several formulas have been proposed to express the elastic modulus of the composite materials by using the moduli of the components. As the simplest formula for the composite with the unidirectional long fiber reinforcements, Nielsen[3] gave a following formula for the longitudinal modulus along the stress direction:

$$E_L = E_m\phi_m + E_f\phi_f \tag{1}$$

where E_m and E_f are the respective moduli of the matrix and the fiber[1] and ϕ_m and ϕ_f are the corresponding volume fractions. In this case, the tensile load extends the fiber and the matrix simultaneously by the same extension and the stress is shared by the components in proportion to their volume fractions.

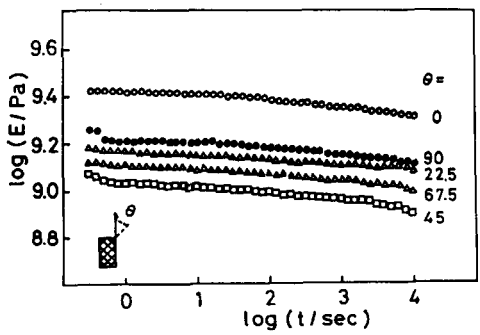

Fig. 6. Relaxation curves for type III composite at various fiber orientation angles.

For the transverse direction of a unidirectionally reinforced composite, the following most general formula for the transverse modulus E_T is given by Lewis and Nielsen[7] as a modification of the formula presented by Halpin[8]:

$$\frac{E_T}{E_m} = \frac{1 + AB\phi_f}{1 - B\psi\phi_f}$$

$$B = \frac{E_2/E_1 - 1}{E_2/E_1 + A}$$

$$\psi = 1 + \frac{1 - \phi_{fm}}{\phi_{fm}^2}\phi_f \tag{2}$$

where $A = 0.5$. ϕ_{fm} is the volume fraction at the maximum packing of the reinforcement and could be taken as 0.82.

The elastic modulus of a composite, which involves fiber reinforcements randomly oriented in a plane, is given by Tsai[5]:

$$E_{2D} \sim (3/8)E_L + (5/8)E_T \tag{3}$$

The moduli for the type I, II, and III composite films at the orientation angles except along fiber axis may be applied by the formula (3).

E_L, E_T, and E_{2D} are plotted against ϕ_f in Figure 7. The relative elastic moduli at 1 s determined from the stress–relaxation curves in reference to E_m obtained for PAI film were also plotted in Figure 7 for type I, II, and III composites at various orientation angles. For type I composite, the relative modulus at $\theta = 0°$ attains a value corresponding to the E_L/E_m line. With the increase of θ, it decreases gradually. Above $\theta = 45°$, the moduli show a little lower value than the E_T/E_m line. For type II, the moduli at 0° and 90° are situated nearly on the E_{2D}/E_m line. Considering that the volume fraction of fibers bearing the load is a half of ϕ_f, the relative moduli should be shifted to the left correspondingly and approaches the E_L/E_m line. Then, the validity of eq. (1) is confirmed in these cases. At $\theta = 45°$, the lowest modulus is found at the point lower than the E_T/E_m line. For type III composite, the relative

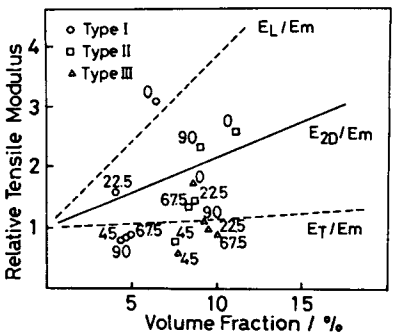

Fig. 7. Relationship of relative modulus with volume fraction of reinforcement for composite films at various orientation angles: (○) type I; (□) type II; (△) type III.

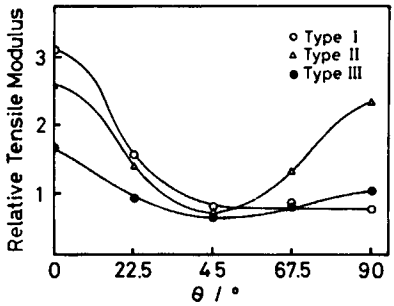

Fig. 8. Relative modulus at 1 s vs. orientation angle for composite film: (○) type I; (△) type II; (●) type III.

moduli at $\theta = 0°$ and 90° are fairly low. Even if the correction for volume fraction bearing the load was considered, the moduli would not reach to the E_L/E_m line. In the cloth reinforcement, the undulated fibers do not directly control the elasticity of the composite. The moduli of type III composites are generally smaller than those of other types. It seems to be the characteristics of the cloth reinforcement.

On the E_{2D}/E_m line based on a random orientation of reinforcement fibers lie the relative modulus for type I at $\theta = 22.5°$, and those for type II at $\theta = 22.5°$ and 67.5°. At these angles, regularly oriented long fibers act the role of randomly oriented short fibers.

In Figure 8, the relative moduli E/E_m at 1 s for composite films are plotted against the fiber orientation angle θ. For type I composite, the relative modulus is greatest at $\theta = 0°$, and is almost the same above 45°. There is a great anisotropy in a plane in this case. For type II at various θ's, the modulus is lower than that for type I at $\theta = 0°$ and lies symmetrically around $\theta = 45°$. Type II composite shows a smaller anisotropy than type I. For type III, the modulus is lowered at $\theta = 0°$. With the cloth reinforcements, the composite becomes more isotropic than with the bidirectional laminate reinforcements. To make the elastic behaviors homogeneous in a plane of the composite materials, tensile modulus E_L must be somewhat sacrificed.

In Figure 8, a great anisotropy in a plane is observed for type I composite. The elastic modulus at an orientation angle θ of the unidirectionally reinforced composite is given by Hoff[9] as follows:

$$\frac{1}{E_\theta} = \frac{\cos^4\theta}{E_L} + \frac{\sin^4\theta}{E_T} + \left(\frac{1}{G_S} - \frac{2\nu}{E_L}\right)\sin^2\theta\cos^2\theta$$

where G_S and ν are the shear modulus and Poisson's ratio, respectively. Assuming $G_S \simeq G_{45}$ (G_S at $\theta = 45°$) and using the relation

$$G_{45} = \frac{E_L E_T}{E_T(1 + 2\nu) + E_L}$$

we have

$$\frac{1}{E_\theta} = \frac{\cos^4\theta}{E_L} + \frac{\sin^4\theta}{E_T} + \frac{E_L + E_T}{E_L E_T}\sin^2\theta\cos^2\theta \tag{4}$$

and the modulus at θ could be calculated from E_L and E_T.

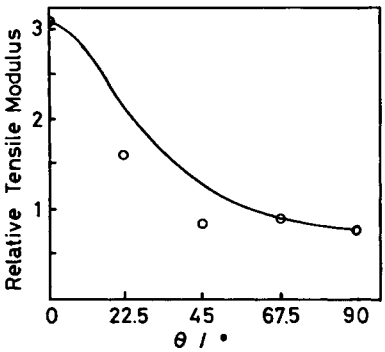

Fig. 9. Relative modulus vs. orientation angle for type I composite film: (——) theoretical curve by eq. (4).

By this procedure, we obtain the relationship of relative modulus E/E_m with θ for type I composite, as shown in Figure 9. By eq. (4), it is expected that the modulus would be considerably lowered by disturbing slightly the arrangement of fibers to the load axis. The experimental data show a more rapid decrease of modulus with increasing θ than expected by eq. (4) and approach a constant above $\theta = 45°$. The difference could be caused by an overestimated contribution of the shear modulus by an assumption of $G_S = G_{45}$. The existence of the more relaxable region around the fibers does not seem to be neglected.

Tensile Load–Elongation

The Kevlar yarns used as a reinforcement showed a brittle fracture at the tensile measurements. The ultimate tensile stress and strain at fracture were 194 kg mm^{-2} and 4.5%, respectively. The homogeneous PAI film exhibited the ultimate stress 6.69 kg mm^{-2} and the strain 12.7%.

In Figure 10 are shown the tensile load–elongation curves obtained for type I composite specimens of a width of 10 mm at various fiber orientation angles. In those measurements it was difficult to estimate the cross sections of the specimens accurately because the thickness of the specimens were not uniform

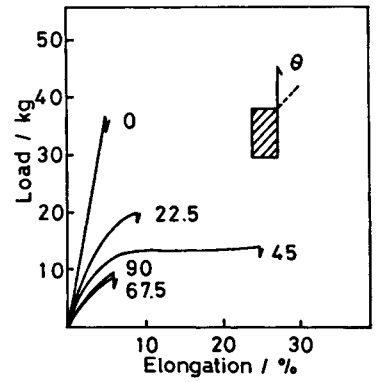

Fig. 10. Tensile load–elongation curves for type I composite film of a width of 10 mm at various fiber orientation angles.

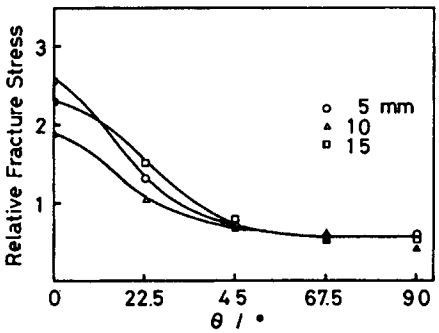

Fig. 11. Fiber orientation dependence of relative tensile fracture stress for type I composite film with various widths (mm) in reference to tensile stress of PAI film: (○) 5; (△) 10; (□) 15.

in the film plane. Then, we plotted the load directly against the orientation angle, instead of plotting the stress. For type I composite, the ultimate load was greatest at $\theta = 0°$ and shows a brittle fracture behavior similar to Kevlar yarns. With increasing θ, the ultimate load decreases and approaches a constant value, as did the stress–relaxation measurements in Figure 4. The elongation was greatest at $\theta = 45°$, showing a ductile character of the type I composite at this fiber orientation in the film plane.

The ratio of tensile fracture load σ and the tensile stress of PAI σ_m is plotted as the relative fracture stress against θ in Figure 11 for type I composite specimen with various widths. Above $\theta = 45°$, the strength does not exceed that of PAI film showing an insufficient reinforcement at these fiber orientations. The dependence on width is found at $\theta = 0°$ and 22.5°. At the same θ, the difference of width of the specimen causes the difference of the effective length of the reinforcement fibers and, in turn, the role of reinforcement.

In Figure 12 are plotted the tensile load–elongation curves for type II composite of a width of 10 mm at various orientation angles. The curves are symmetric around $\theta = 45°$. At $\theta = 0°$ and 90°, brittle fracture behaviors of a high strength were observed showing a dominant role of Kevlar yarns. At the

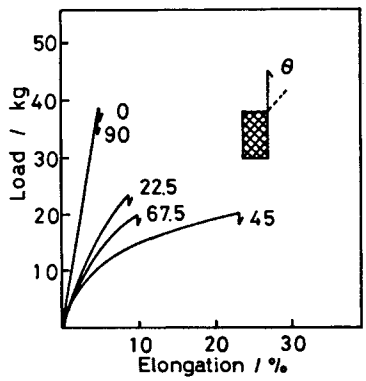

Fig. 12. Tensile load–elongation curves for type II composite film of a width of 10 mm at various fiber orientation angles.

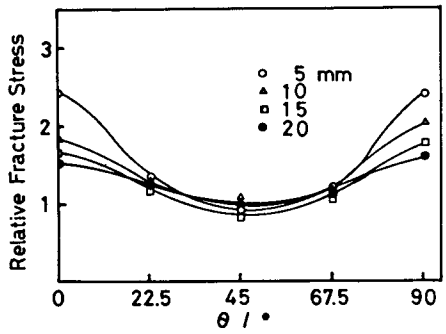

Fig. 13. Fiber orientation dependence of relative tensile fracture stress for type II composite film with various widths (mm) in reference to tensile stress of PAI film: (○) 5; (△) 10; (□) 15; (●) 20.

other orientation angles, the ultimate loads were almost the same. The biggest ultimate strain was found at $\theta = 45°$. Similar behaviors were observed but not shown in figures for specimens of the other widths.

The relative fracture stress is plotted in Figure 13 against the orientation angle for type II composite with various widths. For the specimens of width of 5 mm, the relative fracture stress depends on the orientation angle showing an anisotropy in the film plane. With the increasing width, the ultimate stresses at fiber directions ($\theta = 0°$ and 90°) are lowered and the type II composite becomes apparently isotropic. The effective length of reinforcement fibers is definitely dependent on the width, and the ultimate stress might be investigated with respect to this point.

In Figures 14 and 15, similar plots are shown for type III composite of 15 mm width. At $\theta = 0°$ and 90°, brittle fracture behavior due to Kevlar yarns was observed with a high fracture stress. It is a characteristic for type III composite that the fracture stress is not much dependent on the fiber orientation angle. At orientation angles other than 45°, the ultimate elongation is higher than observed for type I and II composites at the same angle. In Figure 15, we see a small dependence of relative ultimate stress on the

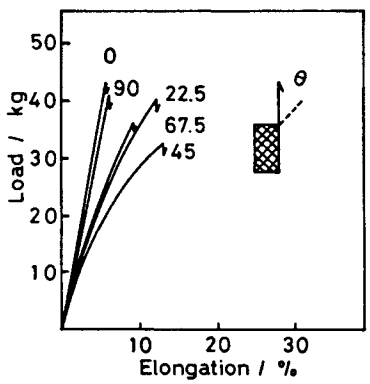

Fig. 14. Tensile load–elongation curves for type III composite film of a width of 15 mm at various fiber orientation angles.

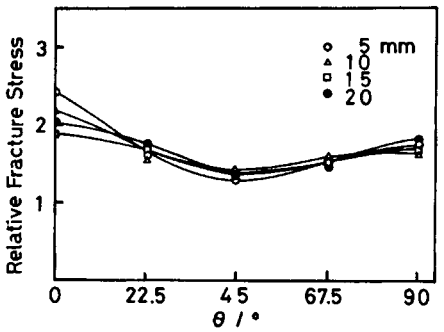

Fig. 15. Fiber orientation dependence of relative tensile fracture stress for type III composite film with various widths (mm) in reference to tensile stress of PAI film: (○) 5; (△) 10; (□) 15; (●) 20.

orientation angle. The type III composite has an overall isotropic character compared with other types.

In Figure 16, relative ultimate stresses at various orientation angles are compared for different types of composite. For type I composite, the relative fracture stress at $\theta = 0°$ is larger than for the other types. With the increase of θ, the relative strength decreases significantly, and it is shown that an anisotropy in the film plane exists in the type I composite. On the other hand, bidirectional reinforcement in type II lowers the relative strength at fiber directions, but more isotropic features are found for this type. The isotropy is achieved with the sacrifice of the strength at the fiber direction. With the bidirectional reinforcement using a plein cloth, type III composite shows a smaller isotropy. The strength at $\theta = 22.5$–$67.5°$ are much enhanced for this type. This is a typical result of a plein cloth reinforcement. The fibers in the cloth are much entangled and constrained with each other. A high strength and isotropy are acquired by these interactions.

Several formulae have been proposed to express the strength of a fiber-reinforced composite by using the strengths of the components. At the longitudinal direction, the strength of the unidirectionally fiber reinforced composite σ_L is expressed by the strength of reinforcement σ_f and that of matrix σ_m as the

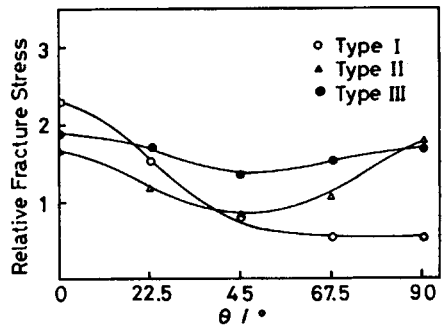

Fig. 16. Fiber orientation dependence of relative tensile fracture stress for various composite films of a width of 15 mm: (○) type I; (△) type II; (●) type III.

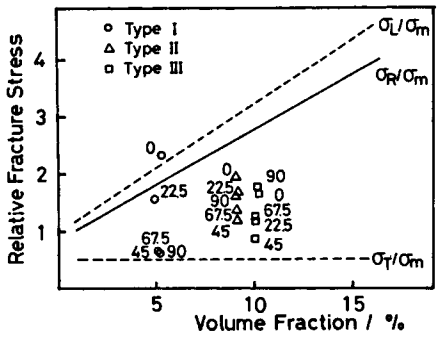

Fig. 17. Relationship of relative tensile fracture stress with volume fraction of reinforcement for various composite films at various orientation angles: (○) type I; (△) type II. (□) type III.

following general formula analogous to the formula for the elastic modulus[3]:

$$\sigma_L = \sigma_f \phi_f + \sigma_m \phi_m \tag{5}$$

where ϕ_f and ϕ_m are volume fractions of reinforcement fibers and of matrix resin, respectively.

For the transverse direction, Nielsen[3] has shown that the strength σ_T is generally smaller than that of the matrix σ_m and is usually approximated by $\sigma_T = \sigma_m/2$.

Riley[10] has shown theoretically that, by involving the discontinuous fibers, the longitudinal strength of the continuous fiber-reinforced composite at the continuous fiber direction σ_R attains at most 6/7 of the original strength σ_L.

In Figure 17, the theoretical relative fracture stresses σ_L, σ_T, and σ_R values are plotted against the volume fraction together with the experimental data. At $\theta = 0°$ for type I composite, σ decreases with the increase of θ and approaches σ_T above $\theta = 45°$, corresponding to a half of σ_m, as Nielsen predicts.

In the fiber directions for types II and III, σ reaches σ_R by the correction of volume fraction. The opposing effects of the transverse fibers cause the lowering of σ. At the other θ's, the fracture stresses are situated between σ_T and σ_R lines, but higher than that for type I composite at $\theta = 45°$. By bidirectional reinforcement, the strength at the fiber directions decreases according to Riley's theoretical prediction, but at the other orientations the strengths are enhanced somewhat.

For the unidirectional reinforcement, Nielsen[3] considered the relationship of the strength and fracture mode in three regions. Between $\theta = 0°$ and 5°, the tensile load is approximately parallel to the fiber direction and the longitudinal strength of the composite determines the fracture mode. Between $\theta = 5°$ and 45°, the shear strength of the composite determines the mode. Above $\theta = 45°$, the mode is determined by the transverse strength of the composite. Considering these factors, Tsai[5] proposed the following formula:

$$\frac{1}{\sigma_\theta^2} = \frac{\cos^4\theta}{\sigma_L^2} + \left(\frac{1}{\sigma_S^2} - \frac{1}{\sigma_L^2}\right)\cos^2\theta \sin^2\theta + \frac{\sin^4\theta}{\sigma_T^2} \tag{6}$$

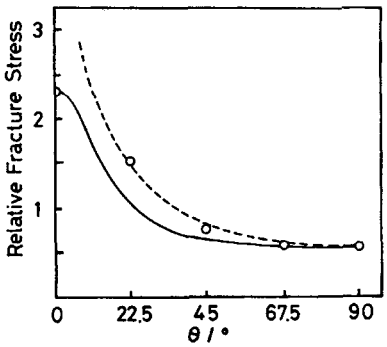

Fig. 18. Relationship of relative tensile fracture stress with orientation angle for type I composite film: (——) theoretical curves by eq. (6); (---) theoretical curve by eq. (7).

where σ_S is the shear strength of the composite, which is approximated by the shear strength of the matrix resin.

The experimental studies of Ishai et al.[11] have shown the following formula which is valid for various composite materials above $\theta = 10°$:

$$\sigma_\theta = \frac{\sigma_T}{\sin \theta} \tag{7}$$

With this model, the fracture strength at directions other than fiber directions is controlled by the transverse strength of the composite. From eqs. (6) and (7), the relationships of fracture stress and orientation angle are plotted in Figure 18. It is expected theoretically that the increase of θ lowers the fracture stress considerably. The experimental data plotted in the same figure show the better coincidence with eq. (7).

The morphology of the fracture surface was investigated with a scanning electron microscope. The observations are shown schematically in Figure 19. For type I composite at $\theta = 0°$, the fibers were broken directly, and some

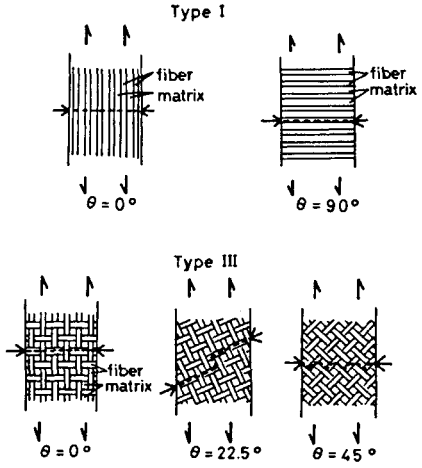

Fig. 19. Schematic descriptions of tensile fracture morphology of type I and III composite films.

fibers were drawn out of the bundles. At $\theta = 90°$, separation of the fiber bundles along fiber directions was observed. For type III at $\theta = 0°$, the longitudinal fibers endure the load directly up to the breakdown as for type I at $\theta = 0°$ and the transverse fibers which do not endure the load are divided with each other in the bundles as for type I at $\theta = 90°$. For type III at $\theta = 22.5°$, the same tendency was observed, i.e., long fibers break directly and short fibers are divided along the fiber axis. For type III composite at $\theta = 45°$, fibers break directly for both directions and cause the overall fracture. If the reinforcing fibers endure the load directly, the fibers act the role of reinforcement effectively to give a high strength and control. If the fibers do not act effectively, the load is endured by the matrix and the strength is lowered. The inside division of the fiber bundles observed in some cases correspond to the large stress relaxation observed for type I composite at $\theta = 90°$.

CONCLUSION

Several informations are obtained for the role of reinforcement fibers in the composite materials and the anisotropy of the composite according to the different composite textures by the measurement of stress–relaxation and tensile load–elongation properties at an ambient temperature. For the unidirectionally reinforced fiber reinforcement, the most effective role of the reinforcement fiber is observed at the fiber direction. The elastic modulus and fracture stress at specimen orientations other than fiber directions are significantly lower. By bidirectional reinforcement is solved the anisotropy problem, but the strength at the fiber directions is depressed markedly by the existence of the fibers of other orientations. The reinforcement by a woven cloth enhances the strength at directions other than fiber directions by the mutual interactions of undulating fibers.

Dr. T. Hiramoto of Film Laboratory, Toray Co., is acknowledged for supplying an experimental sample of PAI varnish. Dr. T. Homma of Tokyo Research Laboratory, Japan Synthetic Rubber Co., is gratified for utilizing an experimental model of Logtimer. Finally, we would acknowledge Mr. Muto and Mr. Tamamura for their collaboration in weaving Kevlar 49 cloth at the Gunma Prefectural Textile Research Institute.

References

1. H. Kambe and K. Oikawa, *J. Soc. Rheol. Jpn.*, **4**, 37 (1976),
H. Kambe, M. Kochi, R. Yokota, K. Oikawa, and H. Gan, *J. Soc. Rheol. Jpn.*, **5**, 35 (1977).
2. Y. W. Mai and F. Castino, *J. Mater. Sci.*, **19**, 1638 (1984).
3. L. E. Nielsen, *Mechanical Properties of Polymers and Composite*, Dekker, New York, 1974, Vol. 2.
4. S. W. Tsai and H. T. Hahr, AFML-TR 78-201 and 79-4040, 1979.
5. S. W. Tsai, AFML-TR 66-149, Parts 1 and 2, 1966.
6. Y. Ohmiya, T. Kawahata, N. Kanai, K. Kuroda, J. Kobayashi, and H. Kambe, *Kobunshi Ronbunshu*, **42**, 905 (1985).
7. T. B. Lewis and L. E. Nielsen, *J. Appl. Polym. Sci.*, **14**, 1449 (1970).
8. J. C. Halpin, *J. Compos. Mater.*, **3**, 732 (1969).
9. N. J. Hoff, *Engineering Laminates*, A. G. H. Dietz, Ed., Wiley, New York, 1949.
10. V. R. Riley, *J. Compos. Mater.*, **2**, 436 (1968).
11. O. Ishai, R. M. Anderson, and R. E. Lavengood, *J. Mater. Sci.*, **5**, 184 (1970).

Received June 19, 1985
Accepted January 9, 1986